ELSEVIER

Chemical Geology 243 (2007) 142–156

CHEMICAL GEOLOGY
INCLUDING
ISOTOPE GEOSCIENCE

www.elsevier.com/locate/chemgeo

The importance of ultrafine particles as a control on the distribution of organic carbon in Washington Margin and Cascadia Basin sediments

L. Coppola [a,b,*], Ö. Gustafsson [b], P. Andersson [a], T.I. Eglinton [c], M. Uchida [c], A.F. Dickens [c]

[a] *Swedish Museum of Natural History, Laboratory for Isotope Geology, Box 50007, 10405 Stockholm, Sweden*
[b] *Stockholm University, Department of Applied Environmental Science, 10691 Stockholm, Sweden*
[c] *Woods Hole Oceanographic Institution, Department of Marine Chemistry & Geochemistry, Woods Hole, MA 02543, USA*

Received 4 May 2006; received in revised form 13 May 2007; accepted 22 May 2007

Editor: J. Fein

Abstract

The combined effects of hydrodynamic particle sorting, sorptive protection and oxygen exposure time (OET) on the distribution of organic carbon in continental margin surface sediments was investigated in detail using the SPLITT fractionation (Split Flow Thin Cell) technique along a well-characterized seven-station transect from the inner Washington shelf to the central Cascadia Basin. The new data highlight the significance of virtually buoyant ultrafine particles (size <38 μm and settling velocity <1 m/d) for organic carbon (OC) deposition. For the entire surface sediment transect, this ultrafine particle fraction hosted 45–85% of the bulk OC, with an increasing contribution further away from the coast. In this fraction, OC to mineral Surface Area (OC:SA) ratios generally ranged from 0.5 to 1.1 mg OC m^{-2}, which is typical of most continental margin sediments, underlining the key role that ultrafine particles undertake in OC sorption. An exception was the lower OC:SA ratios in the <38 μm fraction of Cascadia Basin sediments, which coincided with an order of magnitude increase in Mn oxyhydroxides abundance. An inverse relationship between OC:SA and opal was attributed to a diluting effect of opal on the SA and a lack of association between opal and OC. Finally, two distinct regimes with different preservation controls were revealed along the shelf–slope–basin transect. Finally, the shelf sediments do not follow the relationship between OET and OC:SA observed in the slope and basin sites, presumably due to rapid sedimentation closer to the coast.

Keywords: SPLITT; Carbon preservation; Oxygen exposure time; Carbon accumulation

1. Introduction

The preservation of organic carbon in sediments plays a key role in the global carbon cycle. In order to predict the effects of the recent and ongoing increase in input of atmospheric CO_2 on sedimentary carbon preservation, the processes regulating the distribution of organic carbon in marine sediments need to be better characterized. Research on carbon preservation has traditionally focused on primary controls such as anoxia, high sedimentation rates, and primary productivity. However, recent studies call into question whether these different parameters are

* Corresponding author. Present address: Observatoire Océanologique de Villefranche (OOV), BP 08, 06238 Villefranche-sur-mer, France.
E-mail address: coppola@obs-vlfr.fr (L. Coppola).

0009-2541/$ - see front matter © 2007 Elsevier B.V. All rights reserved.
doi:10.1016/j.chemgeo.2007.05.020

essential for the accumulation of organic carbon-rich deposits (Cowie et al., 1999; Cowie and Hedges, 1993; Kennedy et al., 2002). Indeed, increasing attention has been paid to new concepts of organic matter (OM) preservation, namely protective sorption to mineral surfaces (SA) of otherwise labile OM (Bergamaschi et al., 1997; Bock & Mayer, 2000; Hedges et al., 1997; Keil et al., 1994b; Mayer, 1994b; Ransom et al., 1998) and the oxygen exposure time (OET) (Hedges et al., 1999; Keil et al., 2004; Keil et al., 1998). Mineral surfaces are believed to be important in OC preservation as they may provide physical protection for organic matter against microbial or enzymatic attack (Mayer, 2004). A strong relationship between OC content and mineral SA has been demonstrated for a wide variety of marine sediments (Hedges and Keil, 1995; Mayer, 1994b). Typical OC:SA ratios for most continental margin sediments vary between 0.5 to 1.1 mg OC m^{-2} (Mayer, 1994b) which approximately corresponds to a single molecular monolayer coating. It has been established however that this architecture is unrealistic and it is more likely that organic molecules are unevenly distributed over mineral surfaces (Keil et al., 1994a; Mayer, 1994a; Ransom et al., 1997, 1998).

OET which is a function of sedimentation rate and oxygen penetration depth into the sediment has been shown to strongly influence the burial efficiency for organic matter (i.e. the proportion of OM "raining" onto the seafloor that is buried) (Hartnett et al., 1998; Keil et al., 1994b). A key component of the OET hypothesis is that oxygen exposure eventually leads to the remineralization of OC, regardless of the source or history of the OC. However, recent work of Keil et al. (2004) showed that the regular in situ OET does not include corrections for a portion of the buried organic carbon that may have been exposed to oxygen at a distal location and then laterally transported to the site of burial.

During the off-shelf transport of organic matter, hydrodynamic sorting affects the particle size distribution, with preferential export of fine-grained particles. Consequently, sedimentary particle sizes tend to decrease with increasing distance from the source (Premuzic et al., 1982). In exploring the relationship between SA, OET and OC preservation in marine sediments, the role of the fine-ultrafine fractions is thus of particular importance. Consequently, the pioneering work of Keil et al. (1994a) on the settling velocity of particles in the surface sediments, using SPLITT – split flow thin-cell fractionation – and its relationship with OC sorption deserves further, in-depth, quantitative investigations: this is the central objective of the current study.

River-dominated continental margins provide strong hydrodynamic and geochemical gradients, facilitating investigations of mechanisms of lateral transport and burial of organic matter in marine sediments. Along the Washington continental margin, the depositional environments vary in local primary production, bottom water oxygen concentration, sediment accumulation rate, water depth and fluvial influence (Keil et al., 1994a; Mayer, 1994a, 1994b). This transect has been extensively investigated in terms of its sedimentology (e.g. Landry and Hickey, 1989), and presents large gradients in OC composition and fluxes (Hedges et al., 1999; Keil et al., 2004; Keil et al., 1994a; Prahl et al., 1994). The present study combines for the first time in one coherent investigation the three major carbon preservation concepts of Oxygen Exposure Time (OET), Surface Area (SA) control with emphasis on "ultrafine" component. Geochemical analyses are applied to a more extended inner shelf-deep basin transect than previous studies. It affords quantitative assessment of the role of the ultrafine sediment fraction in dictating the distribution and abundance of organic carbon, and determination of the relative importance of carbon preservation mechanisms in different depositional regimes.

2. Materials and methods

2.1. Study site

The formation of sediment deposits on the Washington mid-shelf is governed by the fluvial sediment load delivered by the Columbia River. The Columbia River is the major source of coarse silts (Nittrouer and Sternberg, 1981). At the mouth of the estuary, sediments are carried northward parallel to the shore by resuspension during winter storms (Kachel and Smith, 1989). It produces a well-defined natural sorting of material into a mid-shelf silt deposit. Previous observations showed that coarse sand and silts emanating from the Columbia River were concentrated over the shelf while the preferential export of fine-grained particles from the shelf resulted in the accumulation of fine silts over the upper slope (Hedges et al., 1999; Keil et al., 1994a). Consequently, the mid-shelf is covered by silt deposit that separates OC-poor modern sand inshore and relict sand offshore (e.g., Hedges et al., 1999).

Surface sediments (0–2 cm) were collected using a multicorer aboard the R/V New Horizon in May–June 2001 at seven stations along a shelf–slope–basin transect from inner Washington Margin (WM) to central Cascadia Basin (CB) (Fig. 1). The water depth of our

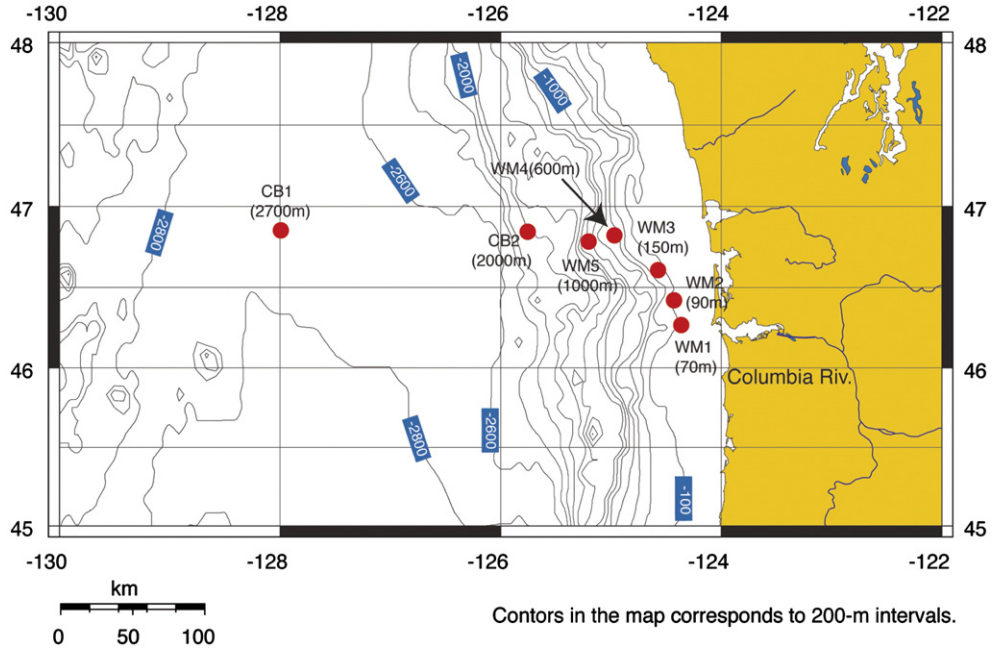

Fig. 1. Location of stations along a transect from the Washington Margin (WM) to the Cascadia Basin (CB). Surfacial sediment samples were collected on the shelf (WM1, 2 and 3), slope (WM4 and 5) and in the open ocean (CB1 and 2).

sampling sites ranges from 70 to 150 m over the shelf (WM1, 2 and 3, respectively), from 600 to 1000 m on the slope (WM4 and 5, respectively), and from 2000 to 2700 m in Cascadia Basin (CB2 and 1, respectively). The shallowest and deepest stations (WM1 and CB1) were respectively 35 and 450 km, west of the Columbia River mouth. These stations were chosen to follow the general trajectory of sediment dispersal from the Columbia River across the shelf and down-slope (Kachel and Smith, 1989; Sternberg and McManus, 1972) and were selected to be in close proximity to sites studied by Keil et al. (1994a), Prahl et al. (1994) and Hedges et al. (1999) where some prior SPLITT analyses (described in Section 2.3) analyses were undertaken and where the OET concept was developed.

2.2. Oxygen penetration depths and sediment accumulation rates

Oxygen penetration depths were measured in sediment cores immediately after sampling using a needle-sized polarographic oxygen electrode (Diamond General, Michigan, USA). The electrode was lowered on the arm of a micro-manipulator through the overlying water and into the sediment in 0.5 mm increments. The electrical current created by the reduction of dissolved oxygen at the cathode is measured by a picoamperemeter and is linearly proportional to the dissolved oxygen concentration (Lambourn et al., 1991). The oxygen penetration depth was the depth at which no oxygen was detectable.

Sediment mixed layer depths and sediment accumulation rates were calculated from ^{210}Pb for stations WM1–WM4 and from ^{14}C of bulk OC for stations WM5-CB1. For the ^{14}C calculation, we are using the differences between the ^{14}C ages at depth rather than the ^{14}C ages themselves because ^{14}C of OC represent the input of sources with disparate ages and histories. Consequently, it doesn't matter if the OC is preaged, as long as it's preaged consistently downcore.

Radiocarbon ages of bulk sedimentary OC were determined at the National Ocean Sciences Accelerator Mass Spectrometry (NOSAMS) facility. Standard AMS sample preparation methods were used (e.g. McNichol et al., 1994). For ^{210}Pb dating, dry sediment (1–2 g) was analyzed for ^{210}Pb (46.5 keV) and ^{214}Pb (351 keV) with a high-purity germanium gamma spectrometer with a closed-end coaxial well (Canberra model GCW 4023S). ^{210}Pb-based sedimentation rates were calculated by fitting the unsupported ^{210}Pb (i.e., total ^{210}Pb–^{214}Pb) using the constant rate of supply (CRS) model (Appleby and Oldfield, 1978).

2.3. SPLITT fractionation

The theory of SPLITT fractionation has been described in previous studies (Giddings, 1985; Keil et al., 1994a;

Gustafsson et al., 2000). The SPLITT instrument uses gravity to separate particles based on their characteristic settling velocities during passage of the suspended sediment through a laminar flow. The settling-velocity-based separation of particles at the exit of the SPLITT thus depends on size, shape, density of the particles, and on the flow rates used with the instrument. The instrumental settling-velocity cutoff was dialed in by adjusting the input and output flow rates of the SPLITT instrument and is described by the equation:

$$U_{\text{cut-off}} = \frac{V(a) - 0.5V(a')}{b \times L} \quad (1)$$

where $V(a)$ and $V(a')$ are the flow rates of the upper outlet and inlet of the SPLITT cell, respectively, while L and b represent the length and breadth of the SPLITT cell (Giddings, 1985). Importantly, it is exactly this property – settling velocity – as opposed to size, that renders SPLITT fractionation so well suited to the study of particle resuspension and lateral transport.

In the present study, we used the Extra High Capacity SPLITT (EHC-SPLITT) instrument that has a throughput capacity 20 times higher (100–500 g/h) than the High Capacity-SPLITT (HC-SPLITT) used in previous applications in marine science (e.g., Keil et al., 1994a, Gustafsson et al., 2000). The EHC separation cell affords rapid (less than 1 h) fractionation of large volumes of sample over a wide range of cutoff settling velocity (0.5 to 7 m/d). Validation of the EHC-SPLITT fractionation method for surface sediments has been described recently by Coppola et al. (2005).

Prior to SPLITT fractionation, the bulk sediments were separated into successively smaller grain size fractions by wet sieving through 250, 100, 63 and 38 μm stainless steel sieves (Fig. 2). The fraction passing through the smallest mesh sieve (<38 μm) was subsequently separated without dispersion chemicals using

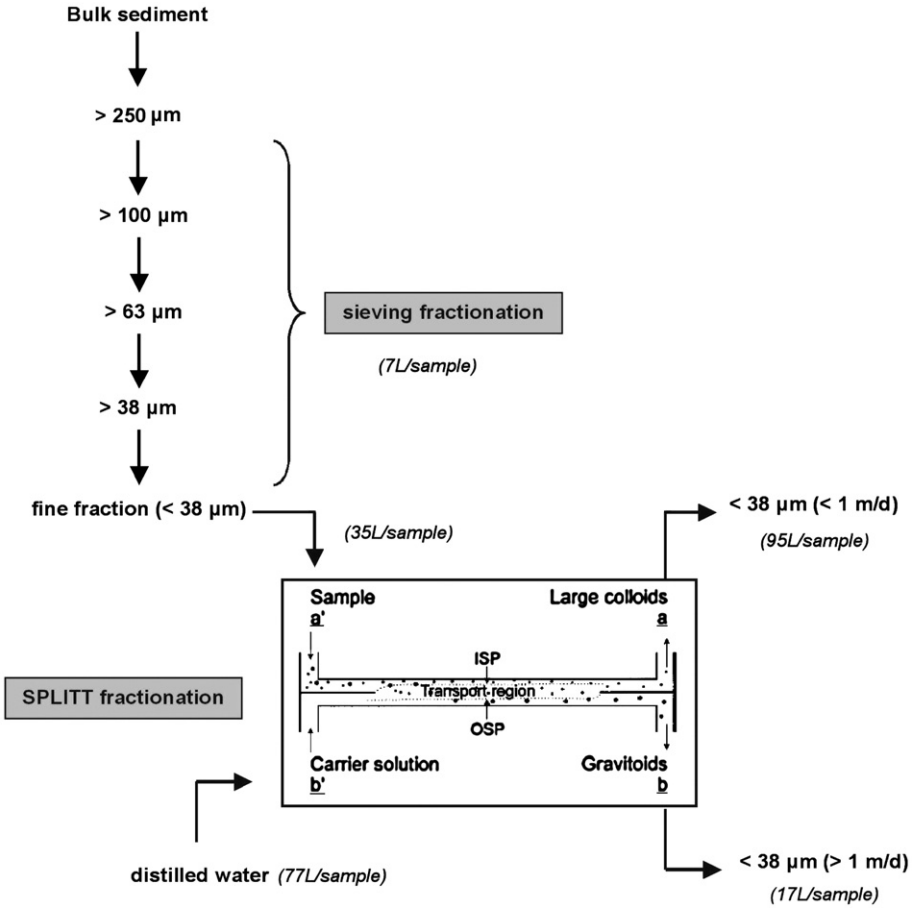

Fig. 2. Sieving and SPLITT fractionation method used to separate the bulk sediment into 6 fractions. Ultrafine particles at the exit of the SPLITT are denoted <38 μm (>1 m/d) and <38 μm (<1 m/d). The values in parentheses represent the water volume used during the experiment.

the EHC-SPLITT fractionation into hydrodynamic fractions using a cutoff settling velocity of 1 m/d (Fig. 2). The two SPLITT fractions were collected and concentrated by ultra-centrifugation (1 h at 10,000 rpm) into a <38 μm (settling velocity >1 m/d) and a <38 μm (settling velocity <1 m/d) fraction. In this paper, the sieve-retained fractions (>38 μm) will be termed "coarse" fractions, whereas the sieve-passing particles (<38 μm) will be termed "fine" fractions. The fine particles that remain virtually buoyant in the SPLITT separation (i.e., <38 μm and settling velocity <1 m/d) are termed the "ultrafines". To allow for comparison with other metrics, if a particle density of 2.4 g/cm^3 and a spherical shape are assumed, this settling velocity corresponds approximately to a size of 4 μm. However, we stress the benefit of a clear physical definition based on both of the intrinsic particle properties size and settling velocity for the characterization of hydrodynamic sorting process. After separation, all particle fractions were air dried (40–50 °C, 48 h) and analyzed for carbon content, mineralogical composition and specific mineral surface area.

2.4. Carbon analysis

Sub-samples of all sieving-SPLITT fractions were analyzed for both the concentration of Total Organic Carbon (TOC) and Total Carbon (TC) by an Europa Scientific IRMS instrument (Isotope Ratio monitoring gas Mass Spectrometer; PDZ Europa, UK). The $CaCO_3$ concentration was calculated by difference of the two. Subsamples slated for TOC analysis were first treated through a repetitive in situ microacidification (1 N HCl) scheme in pre-combusted Ag capsules as outlined in Gustafsson et al. (1997).

2.5. Mineralogy

Minerals were identified by X-ray diffraction (XRD) on oriented mounts of clay-sized particles. XRD diffractograms were obtained using a Philips PW 1710 diffractometer with CuKα radiation and Ni filter, using a high voltage of 40 kV, which yielded an intensity of 25 mA. XRD runs were performed, following air-drying, ethylene–glycol saturation for 12 h and heating at 490 °C for 2 h. Goniometer scans were from 4° to 60° (2θ) for air-dried and glycolated conditions. Identification of minerals was made mainly according to the position of the (001) series of basal reflections on the XRD diagrams. Semi-quantitative estimates of peak areas of the basic reflections were carried out on the glycolated curve using the MacDiff software (Petschick et al., 1996), following the approach of Biscaye (1965). We report the quartz (3.34 Å), albite (3.18 Å) and the main clay mineral groups including smectite (17 Å), mixed-layer clays (15 Å), illite (10 Å), and kaolinite/chlorite (7 Å). Applying the weighting factors of Biscaye (1965; i.e: 4 × the illite peak area, 2 × the kaolinite + chlorite peak area, and 1 × the smectite peak area with the sum normalized to 100%) yields semi-quantitative estimates of relative clay–mineral percentages.

Biogenic silica (opal) analysis was performed at the Large Lakes Observatory (LLO, Duluth, USA) using a timed wet extraction technique with 0.5 M NaOH at 85 °C adapted from De Master (1981). Biogenic silica concentrations are expressed as mg per g dry weight (gdw) of sediment.

2.6. Surface area

The surface area of the mineral grains in all sieve-SPLITT fractions were determined by nitrogen adsorption using a multipoint BET analysis (Clearscience Inc., Minneapolis, USA). Prior to analysis, 1 g of sample was heated in a furnace (350 °C, 24 h) to remove organic matter coating on particles (Mayer, 1994a). Before the surface area measurements, the samples were degassed at 90 °C for one hour and then at 125 °C for 2 h. The surface area is expressed as m^2/g with a relative error from 0.3 to 1.3%.

3. Results

3.1. Mass distribution

The total mass recovery, following sieve and SPLITT fractionation, ranged from 80 to 97% (mean of 90%). The distribution of mass between the different size and settling velocity fractions varies in a systematic way with offshore distance (Table 1; Fig. 3). In the inner shelf region (WM1 and 2), 55–70% of the total mass is contained in the 100–250 μm fraction, and particles >250 μm constitute the most important fraction on the outer shelf (WM3, 150 m depth). On the shelf, only 13–17% of the particle mass is accounted for by the ultrafine fraction (<38 μm and <1 m/d). In contrast, fine particles (e.g. <38 μm) become dominant over the slope (WM4 and 5), comprising 70–90% of total mass, with the majority associated with the ultrafine fraction. This trend of increasing proportions of ultrafine sediment continues offshore into the Cascadia Basin (CB1 and 2) where the fine fraction constitutes 93 and 98% of the total mass, respectively, of which 70–80% is in the ultrafine fraction.

Table 1
Mass, organic carbon, surface area and mineralogical data for each size fraction of sediments

Size fraction (μm)	% mass	TOC (mg/gdw)	SA (m^2/gdw)	$CaCO_3$ (mg/gdw)	$BioSiO_2$ (mg/gdw)	% quartz	% feldspar	% clays	% others
Washington Margin 1 (70 m, 124.3 W, 46.3 N)									
Bulk		8.0±0.5	16.2	15.6±2.0	92.6	–	46	44	10
>250	5	53.0±6.4	3.8	110.4±3.9	7.0	53	19	24	3
100–250	54	0.8±0.0	3.2	n.d.	2.9	8	32	54	5
63–100	4	11.0±3.4	4.8	45.6±1.8	7.8	5	37	15	43
38–63	16	1.3±0.0	3.2	2.6±0.3	5.1	33	14	13	40
<38 (>1 m/d)	5	15.3±3.3	14.8	26.2±2.2	74.7	44	38	18	–
<38 (<1 m/d)	13	26.8±0.9	33.5	15.6±1.0	136.6	29	42	29	–
% recovery	97	96.5							
Washington Margin 2 (90 m, 124.4 W, 46.5 N)									
Bulk		7.5±0.5	6.8	8.7±0.1	26.1	52	28	6	14
>250	1	62.2±0.0	6.6	n.d.	4.5	3	–	85	12
100–250	69	1.9±0.2	3.8	n.d.	4.8	46	28	17	9
63–100	3	5.4±0.2	3.7	n.d.	7.3	51	17	25	6
38–63	3	9.9±0.0	5.4	21.3±0.2	12.3	36	10	51	3
<38 (>1 m/d)	6	11.9±0.5	11.4	n.d.	67.4	35	49	16	–
<38 (<1 m/d)	15	24.1±1.8	29.7	5.1±0.7	158.4	28	33	38	–
% recovery	97	91.0							
Washington Margin 3 (150 m, 124.6 W, 46.7 N)									
Bulk		7.8±0.5	19.2	6.0±0.4	39.6	–	12	67	22
>250	42	2.3±0.1	62.2	n.d.	8.7	–	52	48	–
100–250	16	2.3±0.7	40.9	0.4±0.1	9.2	33	53	14	–
63–100	8	6.2±2.1	9.0	23.5±0.4	9.3	62	–	38	–
38–63	2	7.9±0.1	17.0	n.d.	21.2	–	29	64	6
<38 (>1 m/d)	10	11.1±0.3	18.0	17.7±0.3	92.1	41	32	27	–
<38 (<1 m/d)	17	27.7±0.1	34.6	16.4±0.8	181.0	–	40	60	–
% recovery	94	98.0							
Washington Margin 4 (600 m, 125 W, 46.8 N)									
Bulk		28.2±2.0	16.8	15.4±0.1	107.5	42	25	33	–
>250	0			n.d.	–	–	–	–	–
100–250	0			n.d.	–	–	–	–	–
63–100	3	12.6±0.8	13.9	n.d.	38.9	52	26	17	5
38–63	5	7.9±0.2	8.4	n.d.	23.4		46	54	–
<38 (>1 m/d)	26	17.6±0.8	16.4	15.3±0.1	97.7	52	30	18	–
<38 (<1 m/d)	56	32.5±0.6	30.3	21.6±0.4	160.5	31	43	25	–
% recovery	91	83.4							
Washington Margin 5 (1000 m, 125.2 W, 46.7 N)									
Bulk		18.1±0.2	15.2	4.3±0.4	59.5	56	8	35	–
>250	8	3.0±0.1	31.0	n.d.	9.5	11	57	32	–
100–250	5	6.1±0.0	28.2	n.d.	22.6	36	58	6	–
63–100	5	5.0±0.7	14.0	n.d.	9.6	63	26	7	3
38–63	8	3.7±0.4	7.4	n.d.	18.3	53	32	12	3
<38 (>1 m/d)	23	13.5±0.0	14.6	5.2±0.2	60.4	43	39	17	–
<38 (<1 m/d)	39	28.3±0.6	25.4	26.1±0.1	102.3	25	33	42	–
% recovery	88	84.0							
Cascadia Basin 2 (2000 m, 125.9 W, 46.8 N)									
Bulk		19.1±0.1	23.0	0.4±0.1	147.8	36	18	26	20
>250	0			n.d.	–	–	–	–	–
100–250	0			n.d.	–	–	–	–	–
63–100	0		16.2	n.d.	–	–	–	–	–
38–63	2	13.9±0.8	24.2	n.d.	177.3	58	26	16	–
<38 (>1 m/d)	24	12.1±0.1	37.8	n.d.	145.9	14	18	68	–
<38 (<1 m/d)	59	18.9±2.7		n.d.	188.3	36	15	49	–
% recovery	85	74.1							

(continued on next page)

Table 1 (*continued*)

Size fraction (μm)	% mass	TOC (mg/gdw)	SA (m^2/gdw)	$CaCO_3$ (mg/gdw)	$BioSiO_2$ (mg/gdw)	% quartz	% feldspar	% clays	% others
Cascadia Basin 1 (2700 m, 128 W, 46.7 N)									
Bulk		12.0±0.1	38.2	6.6±0.0	185.1	47	28	13	12
>250	0			n.d.	–	–	–	–	–
100–250	1			n.d.	–	–	–	–	–
63–100	1		32.2	n.d.	–	–	–	–	–
38–63	3	5.9±0.0	46.5	n.d.	467.1	58	34	8	–
<38 (>1 m/d)	13	9.7±0.0	54.0	14.2±0.1	180.1	8	6	85	–
<38 (<1 m/d)	62	14.7±0.0	16.2	10.1±0.5	194.1	19	24	57	–
% recovery	81	87.9							

The mass size distribution is expressed relative to the bulk sediment while Total Organic Carbon (TOC), carbonate ($CaCO_3$) and opal ($BioSiO_2$) are expressed in mg per g of dry weight sediment for each size fraction. Other minerals are expressed as percent of the total response of the XRD analysis. n.d. (no data) indicates that samples were not analyzed and the blank spaces mean not detected.

3.2. Mineralogical composition

The mineral composition of surface sediments varies among size fractions and geographic location (Table 1). Quartz constitutes about half of the total minerals in all samples in terms of total response of the XRD analysis, and is about equally distributed among the >38 μm and <38 μm size fractions. Clays represent the second most abundant group of minerals in all samples with an average of 32% of total XRD response in the bulk. The clay minerals identified in these samples are illite, kaolinite, chlorite and smectite, while feldspar is mainly composed of albite. Clays vary between particle sizes and some variations across the transect were also observed. Among the clays, illite is the main form in the bulk sediments (10–40% in terms of total response of the XRD analysis) and remains predominant in Cascadia Basin stations over the different sediments fractions. In the Washington Margin stations, kaolinite becomes more prevalent in the "less-buoyant" fine (<38 μm and >1 m/d) and ultrafine (<38 μm and <1 m/d) fractions. Feldspar represents 24% on average in the bulk and is generally uniformly dispersed among the size fractions, whereas a significant amount was observed in fine fractions in the Cascadia Basin stations.

Less crystalline minerals that were not amenable to XRD analysis (e.g., carbonates and opal) were analyzed separately. In bulk sediments, carbonate concentrations

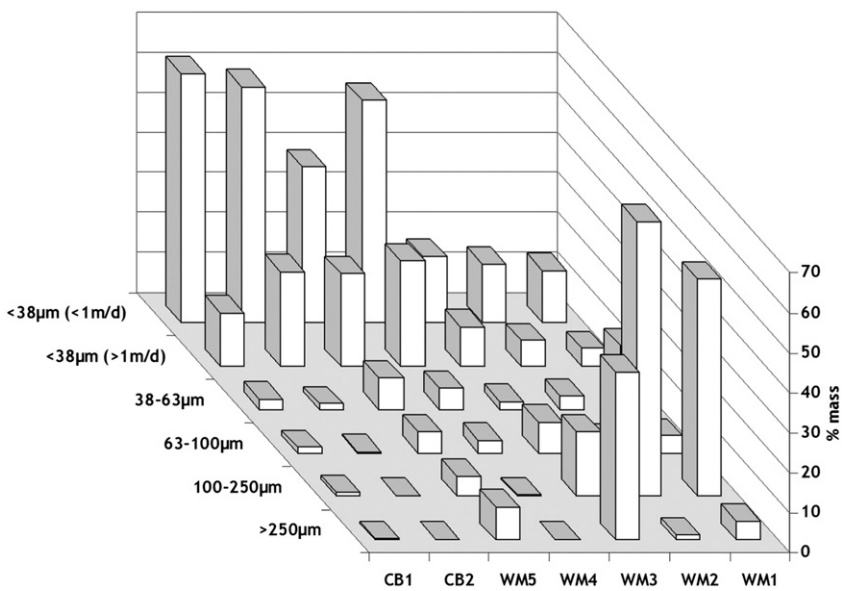

Fig. 3. Distribution of mass among the sieve-SPLITT fractions of the sediment samples. The mass recovery ranges from 80 to 97% (mean of 90%). The uncertainty (expressed as one relative standard deviation) ranges from 1 to 3%.

(0.4–16 mg/gdw) are uniformly low while opal (biogenic silica) concentrations are higher at all stations (26 to 185 mg/gdw). These ranges are similar to those observed by Keil et al. (1994a) for sediments collected from the Columbia River sedimentary plume to the continental slope. They reported bulk sediment carbonate and opal concentrations from 1 to 15 mg/gdw and from 75 to 145 mg/gdw, respectively (Keil et al., 1994a). In our study, the content of carbonates varies also among the size and settling fractions. In shelf sediments, carbonates are more abundant than opal in larger-size fractions whereas on the slope and in the basin, carbonates are only detectable in the <38 μm fractions (Table 1). Overall, the low calcium carbonate concentration in North Pacific sediments is related to carbonate dissolution just below the sediment water interface (Emerson and Bender, 1981). Opal has the opposite distribution to calcium carbonate. For the shelf and slope stations, opal is abundant through all ultrafine fractions (<38 μm and <1 m/d) (102 to 182 mg/gdw). In the Cascadia Basin stations, the opal in larger-size fractions becomes more important and these are dominant at the outermost station CB1 (e.g., 467 mg/gdw in 38–63 μm fraction).

3.3. Organic carbon distribution

TOC content of the bulk sediments ranges from 7.5–8.0 mg/gdw on the shelf, 18.1 and 28.0 mg/gdw over the

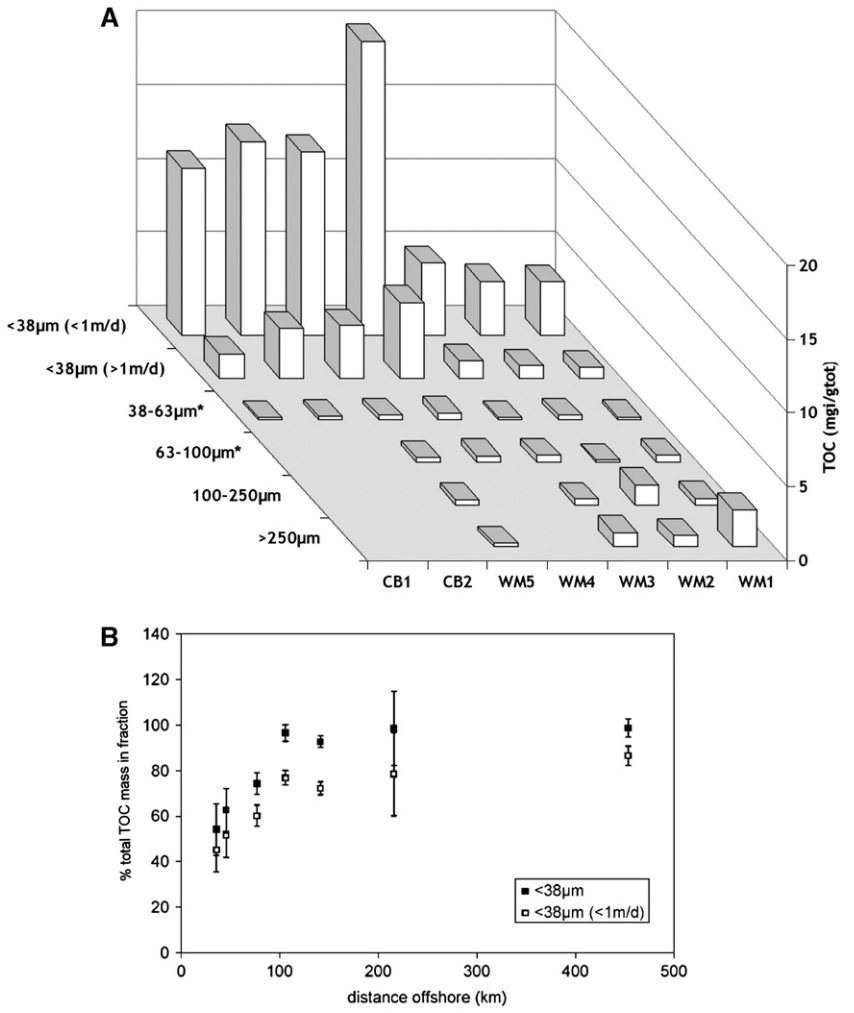

Fig. 4. (A) Distribution of Total Organic Carbon (TOC) among the different fractions in mg of carbon (in size i) per g of total dry weight sediment (mg_i/g_{tot}). It was estimated from TOC concentrations and mass percentage measured in each fractions ($TOC(mg_i/gtot) = TOC(mg/gdw) \times \%mass$). The uncertainty (expressed as one relative standard deviation) ranges from 0.3 to 34%. In the axis label, asterisk symbol for size 38–63 μm and 63–100 μm indicate that for stations CB1/2 and WM4 the correct size range from 38 to >250 μm and from 63 to >250 μm, respectively. (B) Percentage of bulk TOC that exists in the fine (<38 μm) and ultrafine fractions (<38 μm–<1 m/d) versus distance offshore.

slope, to 12.0 and 19.1 mg/gdw in the Cascadia Basin (Table 1). These values are similar to those observed across the shelf and slope by Keil et al. (1994a). A previous study reported that the distilled water used during the SPLITT operation could desorbs as much as 15–20% of the total organic matter (Keil et al., 1994b). In the present study, the high TOC recoveries (88–109% with a mean around 97%) of the entire sieve-SPLITT procedure indicate that OC losses were generally small although they had a measureable effect on the carbon isotopic composition (Uchida et al., in preparation). The distribution of organic matter among the different fractions was estimated from the product of the mass-normalized TOC concentrations in a given fraction and the fraction of the total mass that was apportioned to that same particle fraction: (TOC(mgi/gtot)=(TOC (mgi/gdwi)×%mass (gdwi/gdwtot)). It reveals that OC is overwhelmingly concentrated to the ultrafine fraction (<38 μm and <1 m/d) at each site (Fig. 4A). This ultrafine fraction contains 45–85% of the bulk TOC (Fig. 4A) with an increasing contribution further offshore.

3.4. Mineral surface area

In the present study, the specific surface area (SA) of the bulk sediment samples varies from 7 to 38 m^2/g (Table 2). Surface sediments from the Cascadia Basin stations have generally higher SA values than those from the shelf/slope stations. No clear correlation is apparent between SA and grain size, although SA values from ultrafine particles (<38 μm and <1 m/d) are generally higher than those from the "less-buoyant" fine particles (<38 μm and >1 m/d) (Table 1). We note the high SA recorded for two coarse fractions at WM3, for which we have presently no explanation.

4. Discussion

4.1. Importance of ultrafines for OC distribution

The observed distribution of mass among the sediment size/settling fractions reveals a predominance of the ultrafine range, particularly with increasing offshore distance. This is consistent with the natural process of hydrodynamic sorting of sedimentary particles. The size/settling-fractionated TOC distribution similarly reveals a strong association with fine and ultrafine fractions, particularly with increasing distances offshore (Fig. 4B). Keil et al. (1994a) found the same trend on the shelf and slope, and our analyses demonstrate that it extends out to the lower slope and into the central Cascadia Basin. Our quantitative estimations describe a systematic trend wherein the fraction of TOC residing in the ultrafine fraction – the dominant pool of sedimentary TOC – increases with distance offshore from 45% on the inner shelf to 85% in the abyss (Fig. 4B). Clearly, this specific physical partitioning of sedimentary carbon is impacting transport and other processes controlling the fate of organic matter in the benthic boundary layer and across the sediment–water interface.

The offshore transport of sediment to the continental slope on the Washington Margin region has been estimated to take <1 to 70 yr (Keil et al., 2004). Once suspended, the ultrafine particles may be transported over much greater distances because of their greater buoyancy (<1 m/d) (Thomsen and Gust, 2000). The intermediate and bottom nepheloid layers produced during storms on the Washington continental shelf, as well as bottom currents, underline the potential for resuspension of finer particles from these surface sediments (De Haas et al., 2002).

Table 2
Mixed layer depths, ^{14}C ages of TOC, TOC, mineral specific surface area (SA), sedimentation rate, oxygen penetration depth, oxygen exposure time (OET) and OC accumulation in the bulk surface sediments (0–2 cm)

Station	Water depth (m)	Distance from the coast (km)	mixed layer depth† (cm)	^{14}C age (yr BP)	TOC (mg/gdw)	SA (m^2/g)	Sedimentation rate (cm/kyr)†	oxygen penetration depth (mm)	OET (yr)	OC accumulation ($mg/cm^2/yr$)
WM 1	70	35.5	20	1440±40	8.0	16.2	390±110	6±3	1.5±0.6	3.11
WM 2	90	45.5	27	1300±40	7.5	6.8	320±41	4±1	1.3±0.3	2.26
WM 3	150	76.6	3.5	1370±40	7.8	19.2	290±33	4±1	1.5±0.2	2.36
WM 4	600	105.5	11.5	1550±35	28.2	16.8	110±13	6±1	5.5±0.9	2.85
WM 5	1000	141.1	11.5	1820±25	18.1	15.2	1.4±0.3	4±1	286±71	0.02
CB 2	2000	215.5	3.5	3950±30	19.1	23.0	10.3±1.6	10±3	92±30	0.17
CB 1	2700	453.4	3.5	1670±35	12.0	38.2	3.3±0.4	33±3	1000±86	0.04

The mixed layer depths and sedimentation rate were calculated from ^{14}C data.
† mixed layer depth and sedimentation rates were calculated respectively from ^{210}Pb for stations WM1 to 4 and from ^{14}C for stations WM5, CB2 and CB1.

4.2. Mineral associations of the ultrafine particles

A starting point for evaluating the associations between OC and minerals is to consider the distribution of OC versus the total mineral surface area (SA). In the present study, the OC:SA ratios for all sediment fractions range from 0.3 to 3.8 mg OC m^{-2} (Fig. 5A). For the bulk sediments, the range varies from 0.3 to 1.7 mg OC m^{-2}, which is consistent with estimates from similar locations collated from Keil et al. (1994a) and Hedges et al. (1999). In Fig. 5B, OC and SA data show a generally linear distribution for all samples except for those corresponding to discrete fragments of plant debris deposited on the inner shelf, coarse fractions (>250 μm) and deep basin stations. Although the studied samples reflect a wide variety of depositional conditions and oxygen exposure times, the fine and ultrafine particles, which account for most of the bulk TOC in all sediments, prescribe to a tightly constrained OC:SA trend (Fig. 5C). The deep basin station CB1 and to a lesser extent also, CB2, are exceptions with much lower OC:SA ratios. This may be due to the much higher abundance of Mn oxyhydroxides in the Cascadia Basin sediments. The abundance of MnO in the CB sediments was 3.2–3.6 mg/gdw which is 1–2 orders of magnitude higher than the 0.04–0.4 mg/gdw found in the shelf and slope stations (the authors, manuscript in preparation). Mn oxyhydroxides provide a large specific surface area (e.g., Nelson et al., 1999) but are negatively charged at seawater pH (Appelo and Postma 1999; Tonkin et al., 2004) affording less efficient sorption of at least the portion of OM that is net-negatively charged. This mechanism is thus consistent with the observations of lower OC:SA ratios for CB sediments.

With the exception of a preponderance of kaolinite in the ultrafine fractions in the Washington Margin stations

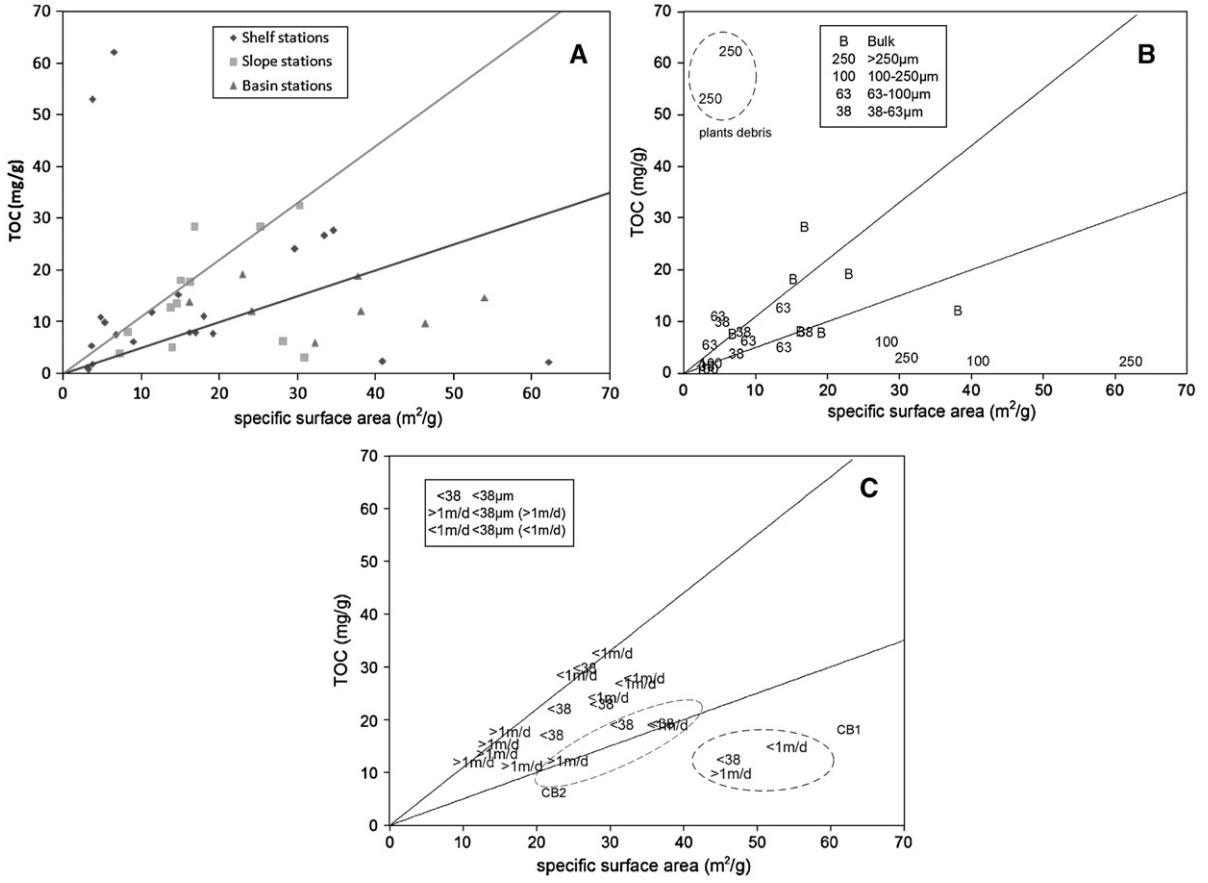

Fig. 5. Total Organic Carbon versus specific mineral Surface Area illustrated for all fractions, labeled according to station location (A), for large fractions (B) and for fine and ultrafine fractions (C). The lines represent the OC:SA ratios typically observed in most continental margin sediments (OC:SA = 0.5–1.1 mg OC m^{-2}) as estimated by Mayer (1994). In diagram B, the dashed circle of data points correspond to plant debris and in diagram C, the dashed circles correspond to data points from deep stations CB1 and CB2, respectively.

(shelf and slope), there was no significant correlation between clays abundance and OC:SA. These results contrast with earlier studies, which suggested that clays play a central role in controlling organic matter preservation (Keil et al., 1994a; Arnarson and Keil, 2001; Kennedy et al., 2002). There was also no relationship between OC:SA ratios and carbonates. This is likely explained by the very low carbonate concentrations in all samples (0.4–15 mg/gdw in the bulk).

The concentration of opal in the bulk fraction is significantly higher than of carbonates and its distribution along the transect presents a larger range (26–185 mg/gdw in the bulk). Opal is most abundant in the fine and ultrafine particles (as it was also seen by Keil et al., 1994a). A significant inverse relationship which exists between OC:SA and opal content in the present data set (Fig. 6A) contrasts with recent suggestions of a quantitatively important role of diatoms bound OC in carbon burial (Ingalls et al., 2003). This inverse relationship in Fig. 6A is not related to an association between opal and OC (Fig. 6C) but instead seems to reflect a significant influence of opal on total SA for ultrafines (Fig. 6B) and also of opal+clays for fine fraction (Fig. 6D) which is consistent with their partitioning in the fine and ultrafine fractions (Table 1).

4.3. Oxygen exposure time and ultrafine carbon

The organic matter that escapes decomposition is buried and preserved in marine sediments. In the carbon preservation process, the role played by the bottom-water O_2 concentration is still unclear. On the one hand, the decomposition of OM is more efficient with oxygen, and hence, organic carbon will be preferentially oxidized in its presence, and preserved in its absence. It has consequently been proposed that oxidation reactions control the distribution and composition of organic matter in slowly accumulating continental slope and basin sediments (Cowie et al., 1995). On the other hand, the kinetics of organic matter decomposition are

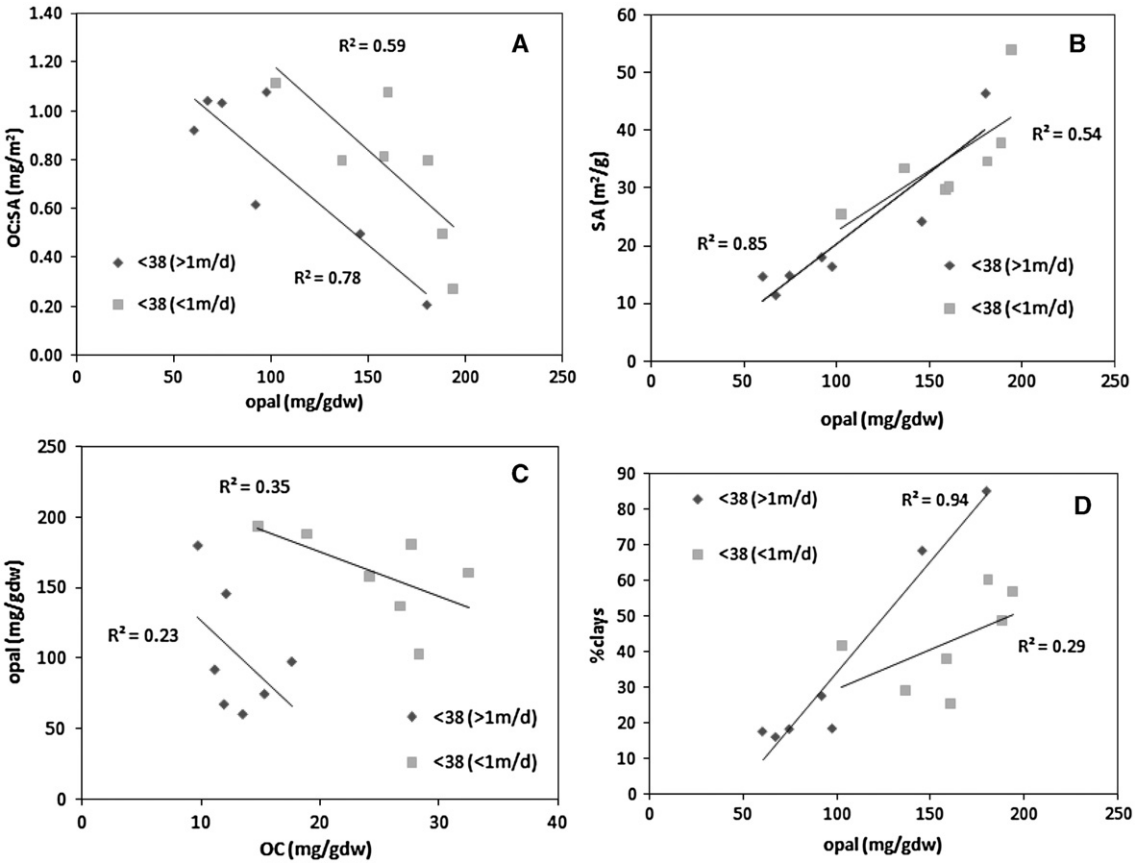

Fig. 6. Distributions for fractions <38 μm (>1 m/d) and<38 μm (<1 m/d) of: (A) OC:SA ratios (mg/m^2) and opal (or bioSiO$_2$) concentrations (mg/gdw), (B) SA (m^2/g) and opal (mg/gdw), (C) opal (mg/gdw) and OC (mg/gdw) and (D) percentage of clays (%) and opal (mg/gdw). The lines in the graph represent the regression (defined with R^2) for each fraction.

similar in the presence and absence of oxygen and there should be no influence of O_2 on preservation. Canfield (1994) suggests that both arguments are correct depending on the circumstances of deposition.

In the Washington Margin, sediments are subject to substantial and prolonged oxic degradation, both during transport to their ultimate burial site and while residing in surface marine sediment horizons (Hedges et al., 1999; Keil et al., 2004). A primary control on the OC degradation in marine sediments is thus believed to be the extent to which organic matter is exposed to molecular oxygen in the water column and sediment pore waters. The concept of Oxygen Exposure Time (OET) was developed as a means to provide quantitative constraints on this process and to examine relationships with OC:SA ratios (Hartnett et al., 1998; Hedges et al., 1999). The OET is quantified as the length of time organic matter is exposed to oxygen and was first defined based on sedimentation rate and oxygen penetration depth into the sediment (i.e., the depth at which molecular oxygen is no longer present).

In this study, mixed layer depths, bulk sedimentation rates and the oxygen penetration depths have been estimated from vertical profiles of ^{210}Pb (WM1–4) and ^{14}C (WM5-CB1) as well as dissolved oxygen, respectively (Table 2). The accuracy of the accumulation rates based on ^{210}Pb and ^{14}C calculations might be critical. For example, Carpenter et al. (1982) observed that Pb-210 sedimentation rates from the Washington coast slope are 2–3 times higher than the true long-term deposition rates. This argues that ^{14}C-based sedimentation rates at WM4 might be more accurate than the Pb-210 rates. However, the sedimentation rates based on ^{14}C and ^{210}Pb agree well at WM4 (82 versus 110 cm/kyr). In addition, sedimentation rates calculated from ^{14}C at WM2 and WM3 are too low (0.08 cm/yr and 0.007 cm/yr, respectively) to agree with previous estimations (Hedges et al., 1999). This suggests that the sedimentation rates based on ^{210}Pb at WM1, 2 and 3 are more realistic than those based on ^{14}C.

The mixed layer depths varied across the transect. In the mid-shelf area (WM1 and 2), ^{210}Pb profiles (full profiles not shown) indicate a mixed layer depth of 20–27 cm (Table 2). In the outer shelf (WM3), the mixed layer depth is very shallow (3.5 cm) and become deeper in the slope area (11.5 cm). This distribution is similar to those observed by Nittrouer et al. (1979) from the ^{210}Pb profiles measured in the same area. In the Cascadia Basin, results indicate a relatively shallow mixed layer depth (3.5 cm). The variations in the mixed layer depth along the transect were not paralleled in the oxygen penetration depth values and thus in the OET data. The estimated OET in the bulk sediments along the transect show that OET increases from 1–2 yr (Washington Margin) to 1000 yr (Cascadia Basin) (Table 2; Fig. 7). For similar locations, Hedges et al. (1999) estimated OET from 38 to 730 yr. Overall, these and prior results demonstrate the presence of two distinct regimes in which different carbon preservation mechanisms dominate (Fig. 7). The slope and basin sites exhibit a strong relationship between sorptive preservation (OC:SA) and OET. In contrast, there appears to be insufficient time on the shelf for such a relationship to become established, and in this regime carbon preservation is instead controlled by rapid sedimentation. An implication of this distinction is that selective preservation is more likely to be observed in the slope and basin regimes, where the TOC is dominantly in the ultrafine particles.

As a result of continuous resuspension and the low settling velocities of organic matter in fluffy aggregates, ultrafine material could reside in the benthic boundary layer for extended period of time, while being laterally transported according to the flow conditions. This type of scenario is consistent with models that describe the surface sediment texture as two-layer system (e.g., Thomsen and Gust, 2000) in which the fluff layer is underlain by a finer and more cohesive sediment that exhibit a higher critical shear stress. The latter parameter is dependent on multiple factors, including particle size distribution, surface roughness, and presence and

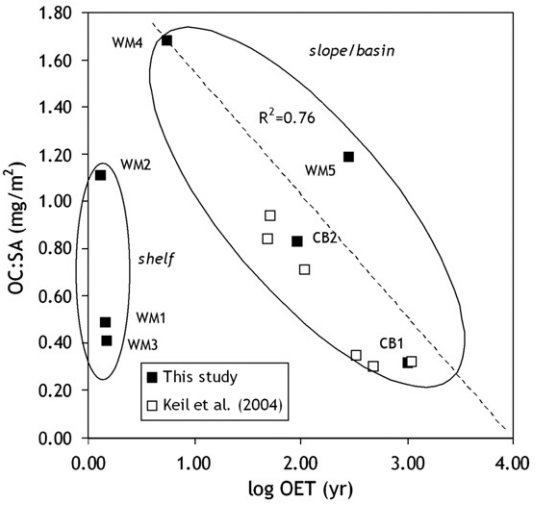

Fig. 7. The OC:SA ratio versus the logarithm of Oxygen Exposure Time (OET) in the bulk sediments. The dashed line represents the negative correlation between OC:SA ratio and log OET with distance offshore for the slope and basin stations. The open square symbols represent the data from Keil et al. (2004) for slope and offshore stations (water depth from 620 to 2750 m) where the OET include the sum of in situ OET and the fractional-transported OET.

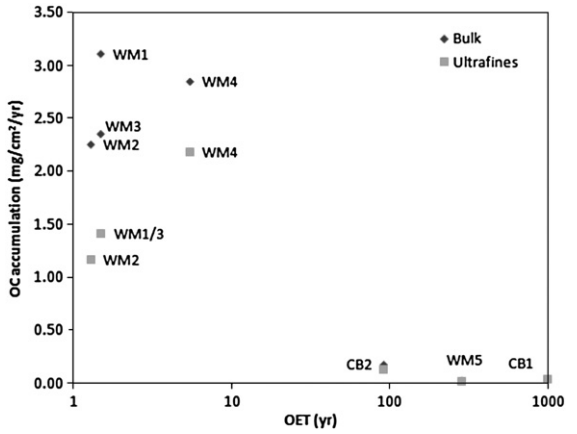

Fig. 8. Organic carbon accumulation (mg/cm^2/yr) versus the log (OET) for the bulk sediments and the ultrafine fractions (<38 μm and <1 m/d). The carbon accumulation was estimated from the TOC concentrations and the sedimentation rates in the surface sediments.

composition of a biological/organic layer. As result, the nepheloid layers produced during storms on the Washington continental shelf, are advected northward along the shelf but also across the shelf (Nittrouer and Wright, 1994). The particles held in suspension in this layer (mainly ultrafines) are thus also advected in the same direction. Depending on the timescales of nepheloid layer transport, this phenomenon could potentially represent an uncertainty in the OET calculation during the lateral dispersal offshore (Keil et al., 2004).

4.4. Role of ultrafine particles in carbon accumulation

Since ultrafine particles play an important role in shaping the TOC distribution (Fig. 4A), they are also likely to strongly influence overall C preservation. Organic carbon accumulation (instead of OC burial since the data is presented here only for surface sediments) accounted for by ultrafine particles was estimated from the contribution of this fraction to the total mass and OC accumulation of bulk sediments. In this study, the overall OC accumulation fluxes in Washington Margin sediments range from 2.3–3.1 (shelf) to 0.02–0.20 (deep basin) mg cm^{-2} yr^{-1}. While these values are low they are quantitatively consistent with previous observations for the Washington Margin (2.4 mg cm^{-2} yr^{-1} in shelf/slope and 0.21 mg cm^{-2} yr^{-1} in deep slope; Devol and Hartnett, 2001), and reflect the inefficiency of carbon accumulation on the Washington Margin where only 1.2% of the primary production escapes oxidation in the surface sediments to be permanently sequestered in sediments (Hartnett and Devol, 2003). Furthermore, the OC accumulation fluxes decrease also with OET and show a large size variation in the Washington shelf sediments (Fig. 8). About half of the bulk OC accumulation fluxes on the shelf is accounted for the ultrafine particles. The importance of the ultrafine fraction increases over the slope sediments and into the basin, reaching 85% of the total OC accumulation in the latter sediments (Fig. 8). This data clearly demonstrates the importance of considering the characteristics and dynamics of the ultrafine particles for furthering the understanding of controlling mechanisms in sedimentary carbon preservation.

5. Conclusions

This study illustrated the influence of particle size-settling velocity and mineralogical composition on the content and accumulation of organic carbon in continental margin sediments off Washington State. Our results are largely supporting the previous suggestion of a coupled influence of surface area and oxygen exposure control on OC accumulation (Keil et al., 1994a; Hedges et al., 1999). Additionally, the results suggest a switch-over in dominating mechanism of carbon preservation between accumulation governed by rapid sedimentation on the shelf and a strong SA–OET relationship in slope and basin regimes. The geochemical characteristics of sedimentary particles suggested that biogenic silica, and Mn oxyhydroxides (basin stations) act to dilute the total SA without a proportional association with OM. Importantly, this study reveals the key role that ultrafine particles (<38 μm and<1 m/d) play in controlling carbon preservation along this shelf–slope–basin transect with 45–85% of bulk OC residing in this ultrafine fraction. Further studies of processes controlling the carbon distribution and preservation in marine sediments may benefit from closer examination of the biogeochemical and hydrodynamic properties of the ultrafine particle fraction.

Acknowledgements

We thank the crew of the R/V New Horizon for their expertise and assistance in collection of the sediment cores. We are grateful to Daniel Montluçon (WHOI) for assistance in sample collection and processing, John Andrews (WHOI) for performing ^{210}Pb measurements, and the NOSAMS facility for radiocarbon analyses We also thank Zofia Kukulska (Stockholm University, Sweden) for technical support and chemical analyses, as well as to A.M. Kähr and U. Hålenius (NRM, Sweden) for instruction and analytical support for the X-

ray diffractometer. We thank John Hayes for advice and comments on an earlier version of this manuscript and Phoebe Lam for discussions on oxydroxides. This research was supported by the Marie Curie Individual Fellowship (MCFI-2002-01383 to L. Coppola). Ö. Gustafsson acknowledges a Senior Researcher Grant from the Swedish Research Council (VR contract no. 629-2002-2309). T. Eglinton acknowledges financial support from NSF (OCE-9907129), and M. Uchida's participation in this project was supported through JAMSTEC.

References

Appelo, C.A.J., Postma, D., 1999. A consistent model for surface complexation on birnessite (MnO_2) and its application to a column experiment. Geochim. Cosmochim. Acta 63 (19/20), 3039–3048.

Appleby, P.G., Oldfield, F., 1978. The calculation of ^{210}Pb dates assuming a constant rate of supply of unsupported ^{210}Pb to the sediment. Catena 5, 1–8.

Arnarson, T.S., Keil, R.G., 2001. Organic–mineral interactions in marine sediments studied using density fractionation and X-ray photoelectron spectroscopy. Org. Geochem. 32, 1401–1415.

Bergamaschi, B.A., Tsamakis, E., Keil, R.G., Eglinton, T.I., Montlucon, D.B., Hedges, J.I., 1997. The effect of grain size and surface area on organic matter lignin and carbohydrate and molecular compositions in Peru margin sediments. Geochim Cosmochim Acta 61, 1247–1260.

Biscaye, P.E., 1965. Mineralogy and sedimentation of recent deep-sea clay in the Atlantic Ocean and adjacent seas and oceans. Geol. Soc. Amer. Bull. 76, 803–832.

Bock, M.J., Mayer, L.M., 2000. Mesodensity organo-clay associations in a near-shore sediment. Mar. Geol. 163 (1–4), 65–75.

Canfield, D.E., 1994. Factors influencing organic carbon preservation in marine sediments. Chem. Geol. 114 (3–4), 315–329.

Carpenter, R., Peterson, M.L., Bennett, J.T., 1982. ^{210}Pb-derived sediment accumulation and mixing rates for the Washington continental slope. Mar. Geol. 48 (1–2), 135–164.

Coppola, L., Gustafsson, O., Andersson, P., Axelsson, P., 2005. Fractionation of surface sediment fines based on a coupled sieve-SPLITT (split flow thin cell) method. Water Res. 39 (10), 1935–1945.

Cowie, G.L., Hedges, J.I., 1993. A comparison of organic matter sources, diagenesis and preservation in oxic and anoxic coastal sites. Chem Geol. 107 (3–4), 447–451.

Cowie, G.L., Hedges, J.I., Prahl, F.G., de Lange, G.J., 1995. Elemental and major biochemical changes across an oxidation front in a relict turbidite: an oxygen effect. Geochim. Cosmochim. Acta 59, 33–46.

Cowie, G.L., Calvert, S.E., Pedersen, T.F., Schulz, H., von Rad, U., 1999. Organic content and preservational controls in surficial shelf and slope sediments from the Arabian Sea (Pakistan margin). Mar. Geol. 161 (1), 23–38.

De Haas, H., van Weering, T.C.E., De Stigter, H., 2002. Organic carbon in shelf seas: sinks or sources, processes and products. Cont. Shelf Res. 22 (5), 691–717.

De Master, D.J., 1981. The supply and accumulation of silica in the marine environment. Geochim. Cosmochim. Acta 45 (10), 1715–1732.

Devol, A.H., Hartnett, H.E., 2001. Role of the oxygen-deficient zone in the transfer of organic carbon to the deep ocean. Limnol. Oceanogr. 46, 1684–1690.

Emerson, S., Bender, M., 1981. Carbon fluxes at the sediment-water interface of the deep-sea; calcium carbonate preservation. J. Mar. Res. 39 (1), 139–162.

Giddings, J.C., 1985. A system based on split-flow lateral transport thin (SPLITT) separation cells for rapid and continuous particle fractionation. Sep. Sci. Technol. 20, 749–768.

Gustafsson, Ö., Haghseta, F., Chan, C., MacFarlane, J., Gschwend, P.M., 1997. Quantification of the dilute sedimentary "soot-phase": implications for PAH speciation and bioavailability. Environ. Sci. Technol. 31, 203–209.

Gustafsson, O., Duker, A., Larsson, J., Andersson, P., Ingri, J., 2000. Functional separation of colloids and gravitoids in surface waters based on differential settling velocity: coupled cross-flow filtration-split flow thin cell. Limnol. Oceanogr. 45 (8), 1731–1742.

Hartnett, H.E., Keil, R.G., Hedges, J.I., Devol, A.H., 1998. Influence on oxygen exposure time on organic carbon preservation in continental margin sediments. Nature 391, 372–374.

Hartnett, H.E., Devol, A.H., 2003. Role of a strong oxygen deficient zone in the preservation and degradation of organic matter: a carbon budget for the continental margins of northwest Mexico and Washington state. Geochim. Cosmochim. Acta 67 (2), 247–264.

Hedges, J.I., Keil, R.G., 1995. Sedimentary organic matter preservation: an assessment and speculative synthesis. Mar. Chem. 49, 81–115.

Hedges, J.I., Keil, R.G., Benner, R., 1997. What happens to terrestrial organic matter in the ocean? Org. Geochem. 27 (5/6), 195–212.

Hedges, J.I., Hu, F.S., Devol, A.H., Hartnett, H.E., Tsamakis, E., Keil, R.G., 1999. Sedimentary organic matter preservation: a test for selective degradation under oxic conditions. Am. J. Sci. 299, 529–555.

Ingalls, A.E., Lee, C., Wakeham, S.G., Hedges, J.I., 2003. The role of biominerals in the sinking flux and preservation of amino acids in the Southern Ocean along 170W. Deep-Sea Res., Part II: Top. Stud. Oceanogr. 50 (3–4), 713–738.

Kachel, N.B., Smith, J.D., 1989. Sediment transport and deposition on the Washington shelf. In: Landry, M.R., Hickey, B.M. (Eds.), Coastal Oceanography of Washington and Oregon. Elsevier, pp. 287–342.

Keil, R.G., Tsamakis, E., Fuh, C.B., Giddings, J.C., Hedges, J.I., 1994a. Mineralogical and textural controls on the organic composition of coastal marine sediments: hydrodynamic separation using SPLITT-fractionation. Geochim. Cosmochim. Acta 58, 879–893.

Keil, R.G., Hu, F.S., Tsamakis, E.C., Hedges, J.I., 1994b. Pollen in marine sediments as an indicator of oxidation of organic matter. Nature 369, 639–641.

Keil, R.G., Tsamakis, E., Giddings, J.C., Hedges, J.I., 1998. Biochemical distributions among size-classes of modern marine sediments. Geochim. Cosmochim. Acta 62 (8), 1347–1364.

Keil, R.G., Dickens, A.F., Arnarson, T., Nunn, B.L., Devol, A.H., 2004. What is the oxygen exposure time of laterally transported organic matter along the Washington margin? Mar. Chem. 92 (1–4), 157–165.

Kennedy, M.J., Pevear, D.R., Hill, R.J., 2002. Mineral surface control of organic carbon in Black Shale. Science 295, 657–660. 25 January 2002.

Lambourn, L.D., Devol, A.H., Murray, J.W., 1991. R/V New Horizon 90–5 cruise report: Water column and porewater data: Seattle, Washington, University of Washington. Special Report, 110. Reference A91–1, p.

Landry, M.R., Hickey, B.M., 1989. Coastal Oceanography of Washington and Oregon. Elsevier Science, Amsterdam.

Mayer, L.M., 1994a. Surface area control of organic carbon accumulation in continental shelf sediments. Geochim. Cosmochim. Acta 58 (4), 1271–1284.

Mayer, L.M., 1994b. Relationships between mineral surfaces and organic carbon concentrations in soils and sediments. Chem. Geol. 114, 347–363.

Mayer, L.M., 2004. The inertness of being organic. Mar. Chem. 92 (1–4), 135–140.

McNichol, A.P., Osborne, E.A., Gagnon, A.R., Fry, B., Jones, G.A., 1994. TIC, TOC, DIC, DOC, PIC, POC-unique aspects in the preparation of oceanographic samples for 14C-AMS. Nucl. Instrum. Methods Phys. Res., B 92, 162–165.

Nelson, Y.M., Lion, L.W., Ghiorse, W.C., Schuler, M.L., 1999. Production of biogenic Mn oxides by leptothrix discophora SS-1 in a chemically defined growth medium and evaluation of their Pb adsorption characteristics. Appl. Environ. Microbiol. 65, 175–180.

Nittrouer, C.A., Sternberg, R.W., Carpenter, R., Bennett, J.T., 1979. The use of Pb-210 geochronology as a sedimentological tool: application to the Washington continental shelf. Mar. Geol. 31 (3–4), 297–316.

Nittrouer, C.A., Sternberg, R.W., 1981. The formation of sedimentary strata in an allochthonous shelf environment: the Washington continental shelf. Mar. Geol. 42 (1–4), 201.

Nittrouer, C.A., Wright, L.D., 1994. Transport of particles across continental shelves. Rev. Geophys. 32 (1), 85–113.

Petschick, R., Kuhn, G., Gingele, F., 1996. Clay mineral distribution in surface sediments of the South Atlantic: sources, transport, and relation to oceanography. Mar. Geol. 130 (3–4), 203–229.

Prahl, F.G., Ertel, J.R., Goni, M.A., Sparrow, M.A., Eversmeyer, B., 1994. Terrestrial organic carbon contributions to sediments on the Washington margin. Geochim. Cosmochim. Acta 58 (14), 3035–3048.

Premuzic, E.T., Benkovitz, C.M., Gaffney, J.F., Walsh, J.J., 1982. The nature and distribution of organic matter in the surface sediments of world oceans and seas. Org. Geochem. 4, 63–77.

Ransom, B., Bennett, R.H., Baerwald, R., Shea, K., 1997. TEM study of in situ organic matter on continental margins: occurrence and the "monolayer" hypothesis. Mar. Geol., 138, 1–9.

Ransom, B., Kim, D., Kastner, M., Wainright, S., 1998. Organic matter preservation on continental slopes: importance of mineralogy and surface area. Geochim. Cosmochim. Acta 62 (13), 29–1345.

Sternberg, R.W., McManus, D.A., 1972. Implications of sediment dispersal from long-term, bottom-current measurements on the continental shelf off of Washington. In: Swift, D.J.P., Duane, D.B., Pilkey, O.H. (Eds.), Shelf sediment Transport: Process and Pattern. Dowden, Hutchinson and Ross, Stroudsburg, pp. 181–194.

Thomsen, L., Gust, G., 2000. Sediment erosion thresholds and characteristics of resuspended aggregates on the western European continental margin. Deep-Sea Res., Part I: Oceanogr. Res. Pap. 47 (10), 1881–1897.

Tonkin, J.W., Balistrieri, L.S., Murray, J.W., 2004. Modeling sorption of divalent metal cations on hydrous manganese oxide using the diffuse double layer model. Appl. Geochem. 19 (1), 29–53.